

# Analytical Methods

Accepted Manuscript

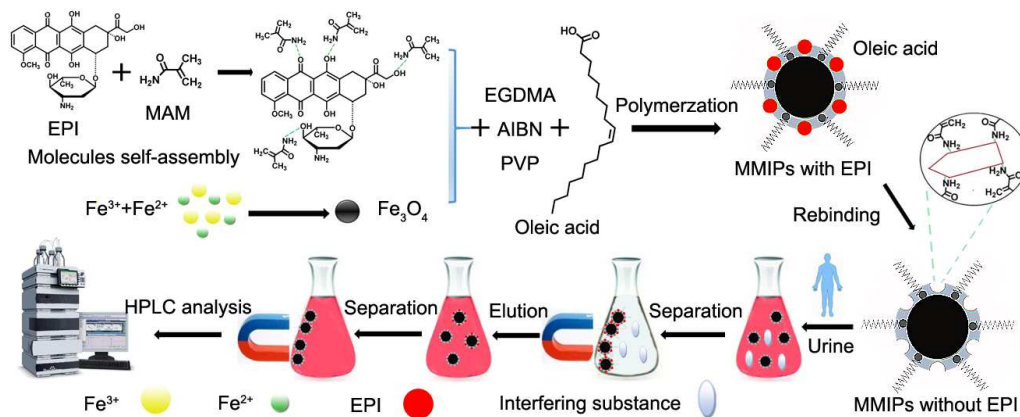


This is an *Accepted Manuscript*, which has been through the Royal Society of Chemistry peer review process and has been accepted for publication.

*Accepted Manuscripts* are published online shortly after acceptance, before technical editing, formatting and proof reading. Using this free service, authors can make their results available to the community, in citable form, before we publish the edited article. We will replace this *Accepted Manuscript* with the edited and formatted *Advance Article* as soon as it is available.

You can find more information about *Accepted Manuscripts* in the [Information for Authors](#).

Please note that technical editing may introduce minor changes to the text and/or graphics, which may alter content. The journal's standard [Terms & Conditions](#) and the [Ethical guidelines](#) still apply. In no event shall the Royal Society of Chemistry be held responsible for any errors or omissions in this *Accepted Manuscript* or any consequences arising from the use of any information it contains.



A detailed discussion was made to explain the adsorption mechanism of the synthesized water-compatible M-MIPs.

1  
2  
3  
4 1 **Simultaneous extraction of anthracyclines from urine using water-**  
5  
6 2 **compatible magnetic nanoparticles with dummy template coupled**  
7  
8  
9 3 **with high performance liquid chromatography**

10  
11  
12  
13 4 Wenyue Zou,<sup>af</sup> Ephraim Mulisa,<sup>af</sup> Lien Ai Pham-Huy,<sup>b</sup> Kai Zhang,<sup>a</sup> Jia He,<sup>a</sup> Chuong  
14 5 Pham-Huy,<sup>c</sup> Deli Xiao,<sup>\*a</sup> Hua He,<sup>\*ade</sup>

15  
16  
17  
18 6

19  
20  
21 7 <sup>a</sup>Department of Analytical Chemistry, China Pharmaceutical University, 24 Tongjia  
22 8 Lane, Nanjing 210009, Jiangsu, China

23  
24  
25  
26 9 <sup>b</sup>Department of Pharmacy, Stanford University Medical Center, Palo Alto, CA, USA

27  
28  
29 10 <sup>c</sup>Faculty of Pharmacy, University of Paris V, 4 Avenue de l'Observatoire, 75006 Paris,  
30 11 France

31  
32  
33 12 <sup>d</sup>State Key Laboratory of Natural Medicines, China Pharmaceutical University,  
34 13 Nanjing 210009, China

35  
36  
37  
38 14 <sup>e</sup>Key Laboratory of Drug Quality Control and Pharmacovigilance, China  
39 15 Pharmaceutical University, Ministry of Education, 24 Tongjia Lane, Nanjing  
40 16 210009, Jiangsu, China

41  
42  
43  
44  
45 17 <sup>f</sup>These authors contributed equally to this work.

46  
47  
48 18 <sup>\*</sup>Corresponding author at: Department of Analytical Chemistry, China Pharmaceutical  
49 19 University, 24 Tongjia Lane, Nanjing 210009, Jiangsu, China Tel.: +86 025  
50 20 83271505; Fax: +86 025 83271505 Email: jcb315@163.com,  
51 21 dochehua@163.com (H He), xiao49562000@163.com (D Xiao)

52  
53  
54  
55  
56  
57 22

58  
59  
60 23

1  
2  
3  
4 24 **Abstract**  
5  
6

7 25 Water-compatible magnetic molecularly imprinted polymers (M-MIPs) for extraction  
8  
9 26 and pre-concentration of anthracyclines (ANTs) from urine have been successfully  
10  
11 27 synthesized by a non-covalent method using epirubicin (EPI) as a dummy template,  
12  
13 28 methacrylamide as a functional monomer, and ethylene glycol dimethacrylate as a  
14  
15 29 cross-linker. The obtained M-MIPs were characterized by scanning electron  
16  
17 30 microscopy (SEM), transmission electron microscopy (TEM), Fourier transform  
18  
19 31 infrared spectroscopy (FT-IR), X-ray diffraction (XRD) and vibrating sample  
20  
21 32 magnetometer (VSM). Adsorption kinetic and isotherm studies were carried out, which  
22  
23 33 indicated that the M-MIPs displayed a rapid dynamic process and a high adsorption  
24  
25 34 capacity. The adsorption behavior was discussed in detail, showing that it could be  
26  
27 35 described as a chemisorption process and both external surface diffusion and intra-  
28  
29 36 particle diffusion contributed to the adsorption mechanism. Furthermore, the binding  
30  
31 37 sites were found heterogeneous for M-MIPs, while homogeneous for M-NIPs. The  
32  
33 38 selectivity of M-MIPs demonstrated higher affinity for target EPI and EPI-analogues  
34  
35 39 over other structurally unrelated compound. A rapid solid-phase extraction (SPE)  
36  
37 40 method using M-MIPs as sorbent coupled with high performance liquid  
38  
39 41 chromatography (HPLC) was established for simultaneous determination of ANTs in  
40  
41 42 urine samples. The recoveries ranged from 93.9%  $\pm$  5.2% to 100.0%  $\pm$  3.4% with the  
42  
43 43 limit of detection of 0.6-2.4 ng mL<sup>-1</sup>. Moreover, the M-MIPs could be regenerated,  
44  
45 44 which could be utilized for several cycles with no obvious decrease in the adsorption  
46  
47 45 capacity. The results indicated that the proposed method is a practical approach for  
48  
49 46 simultaneous determination of ANTs in urine.  
50

51  
52 47  
53  
54  
55  
56 48  
57  
58  
59 49  
60

50

## 1. Introduction

Anthracyclines (ANTs) are widely used as anticancer agents in the treatment of various forms of cancer. Notwithstanding the favorable therapeutic index, their cardiotoxicity is a serious problem. ANTs belong to cytostatic agents which act by either inhibiting cell growth or directly killing cells<sup>1</sup>, their clinical use has been compromised by a cumulative dose-dependent irreversible chronic cardiomyopathy. Therefore, monitoring the concentration and residues of these drugs in the urine of patients is of great significance to determine the correct patient intake. Various methods have been described for the determination of ANTs, including capillary electrophoresis<sup>2, 3</sup>, resonance light scattering<sup>4</sup>, fluorometry<sup>5</sup> and HPLC with different detector<sup>6-11</sup>. Even though some of these methods are sensitive, they require the use of some expensive instruments. HPLC coupled with ultraviolet detector (UVD) as a common apparatus in analytical laboratory is the universal approach to the detection of various drugs. However, it is unsatisfactory for the quantitative determination of ANTs due to their extremely low concentration and the interference of complex matrix in biological fluids. Therefore, enrichment and sample pretreatment processes are required. In order to overcome drawbacks such as time-consuming<sup>12</sup> and solvent-depending<sup>13</sup> of the conventional pretreatment technique, it is necessary to develop a practicable approach with specific recognition and time-saving property for the separation and enrichment of these important anticancer drugs.

Molecularly imprinted polymers (MIPs) as synthetic polymers with cavities which are suitable for the target template molecule and similar compounds, have many advantages such as good recognition property, stability to extreme temperature and pH, flexibility and low cost. They were applied in the drug delivery system of ANTs in recent years<sup>14, 15</sup>. Besides, MIPs have become increasingly attractive in the analytical field as SPE sorbent. The molecularly imprinted-SPE (MISPE) allows the analyte to be pre-concentrated while the interference compounds to be removed from the matrix simultaneously. This technique has been successfully applied in multiple domains<sup>16-18</sup>

1  
2  
3  
4 79 by now. However, the cartridge mode utilized in MISPE is an obstacle in its application  
5  
6 80 due to the tedious column-packing procedure and high back-pressure. When magnetic  
7  
8 81 components are encapsulated into MIPs, the synthesized products, M-MIPs are not only  
9  
10 82 possessing magnetic property, but also have specific and selective recognition property  
11  
12 83 to the template molecule. They are being considered as one of the most popular sorbents  
13  
14 84 for pre-concentration methods of trace analysis<sup>19</sup>. Magnetic-MIPs in SPE can build a  
15  
16 85 controllable extraction process and allow magnetic separation to replace the  
17  
18 86 conventional time-consuming operation<sup>20</sup>. In the magnetic MISPE procedure, M-MIPs  
19  
20 87 can be added into a solution or suspension containing target analytes, then easily  
21  
22 88 separated from the matrix via an external magnetic field, avoiding the process of  
23  
24 89 making packed columns or the additional centrifugation and filtration as in traditional  
25  
26 90 SPE<sup>21-23</sup>.

27  
28  
29 91 However, there is a general concern which relates to the poor level of recognition of  
30  
31 92 the M-MIPs to the analyte in aqueous media. The majority of M-MIPs were synthesized  
32  
33 93 in aprotic and low polar organic solvents. When applied in polar solvents such as water  
34  
35 94 environment, the formation of the pre-polymerization complex during the imprinting  
36  
37 95 procedure can be disturbed, and the hydrogen bonding interactions between template  
38  
39 96 molecules and functional monomers can be destroyed, leading to a lower affinity  
40  
41 97 between M-MIPs and the analyte<sup>24</sup>. Accordingly, application of MIPs in aqueous media  
42  
43 98 is still a challenging and difficult task. In order to obtain MIPs that can selectively  
44  
45 99 recognize the template in aqueous media, it is necessary to exploit other intermolecular  
46  
47 100 interactions, such as ionic interactions<sup>25</sup>, to replace hydrogen bonding interactions.  
48  
49 101 Another widely used approach is the hydrophilic modification on the surface of  
50  
51 102 materials, such as grafting hydrophilic polymeric chains<sup>26</sup> or introducing hydrophilic  
52  
53 103 monomers pre-polymerization<sup>27</sup>. Although a few studies about MISPE in aqueous  
54  
55 104 environment were reported, they basically dealt with the separation and binding  
56  
57 105 performance, there was no detailed knowledge on the adsorption mechanism of MISPE  
58  
59 106 in aqueous media for ANTs. Compared with these methodologies, we proposed a  
60  
107 simple and time-saving solution by utilizing a high amount of oleic acid in the polymer

1  
2  
3  
4 108 synthesis process to make M-MIPs water compatible<sup>14</sup>. Furthermore, a detailed  
5  
6 109 discussion about the adsorption mechanism was conducted.  
7  
8

9 110 In the present work, water-compatible M-MIPs with selective recognition property  
10 111 intended to extract and pre-concentrate ANTs from human urine were prepared. EPI  
11 112 was chosen as dummy template to avoid the inherent bleeding of trace amount EPI  
12 113 when detecting the other ANTs. EPI consists of an aglycone ring coupled to an amino  
13 114 sugar, representing the essential structural features of ANTs. The nature of the structure  
14 115 makes it a suitable dummy template in the recognition of other ANTs. In other words,  
15 116 any compounds with these exact structural features are expected to be recognized by  
16 117 the synthesized EPI-M-MIPs. To the best of our knowledge, it was the first attempt to  
17 118 use a dummy template to prepare M-MIPs as the sorbent of SPE for the rapid  
18 119 simultaneous recognition and extraction of ANTs from aqueous media coupled with  
19 120 HPLC-UV analysis. The M-MIPs obtained were characterized by SEM, TEM, FT-IR,  
20 121 XRD and VSM method. The equilibrium and kinetic data of the adsorption process  
21 122 were then analyzed in detail to study the adsorption kinetic and isotherm of EPI onto  
22 123 the MIPs. The ANTs recognition and separation from spiked urine samples were  
23 124 realized by using M-MIPs as SPE sorbent. Subsequently, by using methanol-acetic acid  
24 125 as elution solution, the two ANTs were selectively extracted from urine samples and all  
25 126 matrix interferences were eliminated simultaneously with satisfactory recovery and  
26 127 high selectivity.  
27  
28  
29  
30  
31  
32  
33  
34  
35  
36  
37  
38  
39  
40  
41  
42  
43  
44

## 45 128 2. Experimental

### 46 129 2.1. Materials

47  
48  
49  
50  
51 130 Epirubicin, Doxorubicin (DOX) and Daunorubicin (DAUN) were purchased from  
52 131 Shandong New Time Pharmaceutical Co., Ltd, China. Gatifloxacin (GTFX) and ferric  
53 132 chloride hexahydrate  $\text{FeCl}_3 \cdot 6\text{H}_2\text{O}$  ( $\text{Fe}^{3+}$ ) were purchased from Sinopharm Chemical  
54 133 Reagent Co., Ltd. (Shanghai, China). Ferrous sulfate heptahydrate  $\text{FeSO}_4 \cdot 7\text{H}_2\text{O}$  ( $\text{Fe}^{2+}$ )  
55 134 and dimethyl sulfoxide (DMSO) were purchased from Nanjing Chemical Reagent Co.,  
56 135 Ltd (Nanjing, China). Methacrylamide (MAM), ethylene glycol dimethacrylate

1  
2  
3  
4 136 (EGDMA), polyvinylpyrrolidone (PVP), azobisisobutyronitrile (AIBN), and oleic acid  
5  
6 137 were obtained from Aladdin Industrial Corporation (Shanghai, China).  
7  
8 138 Sodiumdihydrogen phosphate  $\text{NaH}_2\text{PO}_4 \cdot 2\text{H}_2\text{O}$  was purchased from Shanghai Lingfeng  
9  
10 139 Chemical Reagent Co., Ltd (Shanghai, China) and the phosphoric acid was obtained  
11  
12 140 from Nanjing Chemical Reagent Co., Ltd (Nanjing, China). All these chemicals and  
13  
14 141 solutions used were of analytical reagent grade. Methanol and acetonitrile of HPLC  
15  
16 142 grade were purchased from Jiangsu Hanbon Sci.&Tech. Co., Ltd (Huaian, China) and  
17  
18 143 Nanjing Chemical Reagent Co., Ltd (Nanjing, China), respectively. Ultrapure water  
19  
20 144 was prepared by using an ultrapurification system (Chengdu, China) and used  
21  
22 145 throughout the experiments.

## 23 24 25 146 2.2. *Instruments and HPLC analysis*

26  
27  
28 147 To characterize the nanomaterials synthesized, S-3000 scanning electron microscopy  
29  
30 148 (SEM, Hitachi Corporation, Japan) and a FEI Tecnai G2 F20 transmission electron  
31  
32 149 microscope (TEM) were used to examine the size and the morphology of the  
33  
34 150 nanomaterials. Their surface functional groups were measured with a 8400s FT-IR  
35  
36 151 spectrometer purchased from Shimadzu (Kyoto, Japan). The X-ray powder diffraction  
37  
38 152 pattern (XRD) was performed using X' TRA X-ray diffractometer with  $\text{Cu } K\alpha$   
39  
40 153 irradiation at  $\lambda = 0.1541 \text{ nm}$  for phase identification. To confirm the magnetic properties,  
41  
42 154 tests were done using a LDJ 9600-1 vibrating sample magnetometer (VSM) operating  
43  
44 155 at room temperature with applied fields up to 10 kOe.

45  
46  
47  
48 156 HPLC analysis system consisted of a quaternary pump G1311C, an auto liquid  
49  
50 157 sampler (SLA) G1329B, a column thermostat G1316A and an ultraviolet detector  
51  
52 158 G4212B. Chromatographic separations were carried out using a column purchased from  
53  
54 159 Agilent Technologies (Waldbronn, Germany) (type Eclipse Plus C18,  $3.5 \mu\text{m}$ ,  $4.6 \text{ mm}$   
55  
56 160  $\times 100 \text{ mm}$ ), with column temperature operated at  $30 \text{ }^\circ\text{C}$ . The detection was at  $\lambda = 254$   
57  
58 161  $\pm 2 \text{ nm}$ , reference  $\lambda = 360 \pm 2 \text{ nm}$ . The data were acquired and processed by means of  
59  
60 162 HP ChemStation for LC software. The mobile phase was a mixture of phosphate buffer



1  
2  
3  
4 163 (1%, pH 2.35)-methanol-acetonitrile (60:20:20, v/v/v). The injection volume was 10.0  
5  
6 164  $\mu\text{L}$ , and the mobile phase flow rate was kept constant at  $1.0 \text{ mL min}^{-1}$ .  
7

### 8 9 165 2.3. *Synthesis of M-MIPs*

10  
11  
12 166 The preparation of  $\text{Fe}_3\text{O}_4$  was performed by a chemical co-precipitation of  $\text{Fe}^{2+}$  and  
13  
14 167  $\text{Fe}^{3+}$  ions following our previous report<sup>28</sup>. The experimental procedure was described  
15  
16 168 in Electronic Supplementary Information Appendix S1. Subsequently, the M-MIPs  
17  
18 169 were prepared using the synthesized  $\text{Fe}_3\text{O}_4$  magnetic nanoparticles. The mixture of EPI  
19  
20 170 (1.0 mmol) and MAM (9.0 mmol) dissolved in DMSO (10.0 mL) was stirred for 0.5 h  
21  
22 171 to prepare the preassembly solution.  $\text{Fe}_3\text{O}_4$  (1.0 g) was mixed with DMSO (5.0 mL)  
23  
24 172 under ultrasound for 10 min. Then EGDMA (20.0 mmol) and the preassembly solution  
25  
26 173 were both added into the mixture of  $\text{Fe}_3\text{O}_4$  in DMSO. This mixture was treated by  
27  
28 174 ultrasound again for 0.5 h to prepare the pre-polymerization solution. PVP (0.4 g) was  
29  
30 175 dissolved into 100 mL of DMSO:  $\text{H}_2\text{O}$  (9:1, v/v) in a three-necked round-bottomed  
31  
32 176 flask. The mixture was stirred at 300 rpm and purged with nitrogen gas to displace  
33  
34 177 oxygen at  $60 \text{ }^\circ\text{C}$ . The pre-polymerization solution was then transferred into a three-  
35  
36 178 necked flask followed by adding AIBN (0.1 g). Two hours later, oleic acid (5.0 mL)  
37  
38 179 was added to the flask. After reaction at  $60 \text{ }^\circ\text{C}$  for 12 h, the polymers obtained were  
39  
40 180 separated, and washed by interchanging water with the mixture of methanol: acetic acid  
41  
42 181 (8:2, and 6:4, v/v) several times under ultrasound until EPI could not be detected by  
43  
44 182 HPLC. Finally, the polymers collected were dried in vacuum at  $60 \text{ }^\circ\text{C}$ . The EPI-M-  
45  
46 183 MIPs obtained could be used directly as sorbent for magnetic SPE. In parallel, the  
47  
48 184 magnetic non-imprinted polymers (M-NIPs) were prepared in a similar way to above  
49  
50 185 and used as control, but without adding EPI.  
51

### 52 53 54 186 2.4. *Adsorption kinetic study*

55  
56  
57 187 In adsorption kinetic experiment, 5.0 mg of M-MIPs or M-NIPs was mixed with 50.0  
58  
59 188 mL of EPI solution at a concentration of  $10.0 \mu\text{g mL}^{-1}$  and incubated at room  
60  
189 temperature for 3 h with shaking. After different time intervals (from 0 min to 180 min),

1  
2  
3  
4 190 the sorbent with captured EPI was separated from the suspension with a magnet and the  
5  
6 191 supernatant was then analyzed by HPLC analysis. According to the concentration of  
7  
8 192 EPI before and after adsorption respectively, the amount of EPI bound to M-MIPs or  
9  
10 193 M-NIPs was calculated following equation (1):  
11

$$13 \quad 194 \quad Q = (C_0 - C_t) \cdot \frac{V}{m} \quad (1)$$

16  
17 195 where  $C_0$ ,  $C_t$ ,  $V$  and  $m$ , represent the concentration ( $\mu\text{g mL}^{-1}$ ) of EPI in solution before  
18  
19 196 and after the adsorption process, the volume of the solution (mL) and the weight of the  
20  
21 197 polymer (mg), respectively. The average results from triplicate independent results  
22  
23 198 were used for the following discussion.  
24

#### 25 26 199 2.5. Adsorption isotherm study

27  
28  
29 200 Static equilibrium adsorption tests were performed by suspending 4.0 mg of polymers  
30  
31 201 (M-MIPs or M-NIPs) in 4.0 mL of EPI solution with different concentrations ranging  
32  
33 202 from  $5.0 \mu\text{g mL}^{-1}$  to  $50.0 \mu\text{g mL}^{-1}$ . The screw-capped centrifuge tubes were used as  
34  
35 203 batch reactor systems. All tubes were sealed and executed with ultrasonic-processing  
36  
37 204 for 5 min. Then the mixture was kept for 2 h at room temperature with shaking. After  
38  
39 205 that the mixture was separated by an external magnet. The concentration of free EPI in  
40  
41 206 the supernatant was measured by HPLC analysis. The amount of EPI bound to M-MIPs  
42  
43 207 or M-NIPs was calculated by Eq. (1).  
44

#### 45 46 208 2.6. Selectivity study

47  
48  
49 209 A standard mixture solution of EPI, DOX, DAUN and GTFX with an initial  
50  
51 210 concentration of  $20.0 \mu\text{g mL}^{-1}$  was prepared. 4.0 mg of M-MIPs or M-NIPs was mixed  
52  
53 211 with 4.0 mL of the mixture solution, respectively. The adsorption process was  
54  
55 212 conducted as described earlier for the adsorption isotherm experiments.  
56  
57

#### 58 59 213 2.7. Optimization of SPE procedure

60

1  
2  
3  
4 214 Conditions affecting the performance of the extraction, such as the amount of M-MIPs,  
5  
6 215 the adsorption time and the elution solvent, were investigated to achieve high recovery  
7  
8 216 for ANTs. The SPE procedure was optimized by analyzing spiked DOX and DAUN in  
9  
10 217 urine samples ( $10.0 \mu\text{g mL}^{-1}$ ). Different amount of M-MIPs ranging from 0.5 to 4.0 mg,  
11  
12 218 adsorption time from 10 to 90 min and a variety of elution solvents including water,  
13  
14 219 methanol and methanol: acetic acid (9:1, 8:2, 6:4, v/v) were established. When one  
15  
16 220 parameter was changed, the other ones were kept at their optimal values.  
17

### 18 19 221 2.8. Determination of two ANTs in urine sample

20  
21  
22 222 For the selective recognition and extraction of ANTs from urine sample, a 4.0 mL  
23  
24 223 aliquot of urine from non-treated human sources spiked with DOX and DAUN at the  
25  
26 224 final concentration of 0.1, 1.0 and  $10.0 \mu\text{g mL}^{-1}$  was prepared and loaded onto 3.0 mg  
27  
28 225 M-MIPs and M-NIPs, respectively. After incubation for 2 h at room temperature, M-  
29  
30 226 MIPs and M-NIPs were removed by a permanent magnet and washed with 4.0 mL of  
31  
32 227 water. Then 1.0 mL mixture of methanol: acetic acid (8:2, v/v) was used to elute ANTs  
33  
34 228 adsorbed. The eluted solution was concentrated in vacuum. After that, the residue was  
35  
36 229 dissolved in 0.4 mL mobile phase. Finally, the treated samples were analyzed by HPLC.  
37

### 38 39 230 2.9. Reusability of M-MIPs

40  
41  
42 231 The adsorption-desorption cycle was repeated 5 times by using the same imprinted  
43  
44 232 material in order to show the reusability of the M-MIPs. The adsorption process was  
45  
46 233 conducted as described earlier for the adsorption isotherm experiments. The desorption  
47  
48 234 process was implemented as the washing procedure after the polymerization.  
49

## 50 51 52 235 3. Results and discussion

### 53 54 236 3.1. Synthesis of M-MIPs

55  
56  
57 237 The synthetic approach comprised the following steps: (1) preparation of  $\text{Fe}_3\text{O}_4$  core;  
58  
59 238 (2) self-assembly of the template molecule (EPI) and functional monomer (MAM); (3)  
60  
239 polymerization of the pre-polymeric mixture on the surface of  $\text{Fe}_3\text{O}_4$  core in the

1  
2  
3  
4 240 presence of cross-linker (EGDMA), initiator (AIBN), dispersant agent (PVP),  
5  
6 241 dispersing medium (DMSO) and a special additional agent (oleic acid); (4) eluting  
7  
8 242 template molecule (EPI) with a series of washing process.  
9

10  
11 243 The self-assembling process between template molecule and functional monomer is  
12  
13 244 a key step in the preparation of MIPs. High strength of the complex formed between  
14  
15 245 the template and the monomer represents an essential condition to obtain polymers with  
16  
17 246 good specificity and affinity. Hydrogen bonds, belonging to the non-covalent forces,  
18  
19 247 play a leading role in the self-assembling process. MAM is a reliable functional  
20  
21 248 monomer for EPI<sup>14</sup>. The amide group of MAM is the main part in the hydrogen bond  
22  
23 249 formation because it can interact with both hydrogen bond receptor and donor of EPI.  
24  
25 250 The nitrogen atom of MAM amide group can form hydrogen bond with the hydrogen  
26  
27 251 atom of EPI hydroxide group. Moreover, it is possible to donate two hydrogen atoms  
28  
29 252 to form hydrogen bonds with oxygen atoms of EPI. This ability of MAM makes it  
30  
31 253 possible to obtain heterogeneous binding sites of EPI template on the imprinted polymer.  
32  
33

34 254 The oleic acid acts as an anionic surfactant which contains carboxylic group and  
35  
36 255 could provide a large amount of negatively charged functional groups on the surface of  
37  
38 256 MIPs. These carboxylic groups and the positive metal ions such as ferric ions of the  
39  
40 257 magnetic particles in the system would interact through electrostatic attraction. By this  
41  
42 258 means the MIPs are grafted onto the magnetic particles. After the reaction with the  
43  
44 259 carboxylic groups of oleic acid, there are hydrophobic carbon chains existing outside  
45  
46 260 the template molecule-functional monomer polymer, which can prevent H<sub>2</sub>O molecule  
47  
48 261 from going inside to destroy the hydrogen bond when the polymer is dissolved in  
49  
50 262 aqueous media.  
51

52  
53 263 In order to acquire M-MIPs with high selective recognition and adsorption capacity,  
54  
55 264 the synthesis conditions such as the polymerization time and temperature played  
56  
57 265 important roles. According to our previous research<sup>29</sup>, the polymerization time and  
58  
59 266 temperature were controlled at 12 h and 60 °C to obtain M-MIPs with appropriate  
60  
267 thickness and particle size.

### 268 3.2. Characterizations

269 The FT-IR spectra (Fig. S1), XRD patterns (Fig. S2) and their explanations reported in  
270 Electronic Supplementary Information Appendix S1 and S2 indicate the successful  
271 preparation of the M-MIPs or M-NIPs shell on the surface of iron oxide beads.

272 The SEM image in Fig. 1a at 300 nm and TEM image in Fig. 1b at 100 nm show the  
273 morphology features of the resulting materials. Some agglomerations can be observed  
274 in Fig. 1a and among them exist large cavities. The porosity plays a significant role in  
275 adsorption and elution processes by increasing the adsorption capacity when  
276 recognizing the analytes and improving the mass transfer rate when rebinding them.  
277 From Fig. 1b, it can be observed that the materials are uniform spheres with the size  
278 inferior to 500 nm.

279 Figure 2a shows the hysteresis loops of the magnetite particles recorded at room  
280 temperature. The magnetic saturation ( $M_s$ ) values are 51.62 and 10.17 emu g<sup>-1</sup> for the  
281 Fe<sub>3</sub>O<sub>4</sub> and M-MIPs, respectively. The decrease in the magnetization value from the pure  
282 iron oxide to M-MIPs can be attributed to the coating process around the Fe<sub>3</sub>O<sub>4</sub>, the  
283 magnetically inactive shell has shielded the magnetite. Comparing with the values  
284 reported in other articles<sup>30, 31</sup>, this M-MIPs can be considered to exhibit superior  
285 magnetic property. As shown in Fig. 2b, M-MIPs still remained strongly magnetic to  
286 meet the need of magnetic separation. It can be easily isolated from the aqueous solution  
287 within a few seconds by placing an external magnetic field near the glass bottle and the  
288 supernatant is colorless.

### 289 3.3. Adsorption kinetic study

290 The initial concentration of EPI solution was 10.0 µg mL<sup>-1</sup>. The adsorption time range  
291 was from 0 min to 180 min. Figure 3 indicates the procedure of the adsorption kinetic  
292 of EPI solution onto M-MIPs and M-NIPs. As to M-MIPs, the adsorption amount  
293 increased with the time in the first 50 min then remained stable in the following time.  
294 Obviously, the adsorption amount of M-NIPs was smaller. In addition, M-NIPs were

1  
2  
3  
4 295 easier to reach equilibrium. It was less than 20 min for them to get the maximum  
5  
6 296 adsorption amount. It means that, there were imprinted cavities and specific binding  
7  
8 297 sites existing inside the M-MIPs, which can recognize the template molecule and its  
9  
10 298 analogues. In the first 50 min, they took up the cavities and sites gradually, resulting in  
11  
12 299 the increasing of the adsorption amount. But for M-NIPs, there was no such imprinted  
13  
14 300 cavity or specific binding site. EPI molecules were adsorbed on the surface of M-NIPs,  
15  
16 301 the binding site was limited. So the adsorption amount was low and the equilibrium was  
17  
18 302 easy to be got.

19  
20  
21 303 In our study, two different models: pseudo-first-order model and the pseudo-second-  
22  
23 304 order model were used to further analysis of the adsorption process, and intra-particle  
24  
25 305 diffusion model was used to examine the adsorption mechanism.

26  
27  
28 306 The pseudo-first-order model is described as:

29  
30  
31 307  $\ln(Q_e - Q_t) = \ln Q_e - K_1 t$  (2)

32  
33  
34 308 where  $Q_e$  and  $Q_t$  represent the amount ( $\mu\text{g mg}^{-1}$ ) of EPI adsorbed at equilibrium and  
35  
36 309 time  $t$  (min), respectively, and  $K_1$  is the rate constant for pseudo-first-order. A straight  
37  
38 310 line from a plot of  $(Q_e - Q_t)$  versus  $t$  should be obtained if the model is applicable.

39  
40  
41 311 The pseudo-second-order model is described as:

42  
43  
44 312  $\frac{t}{Q_t} = \frac{t}{Q_e} + \frac{1}{K_2 Q_e^2}$  (3)

45  
46  
47 313 where  $Q_e$  and  $Q_t$  refer to the amount ( $\mu\text{g mg}^{-1}$ ) of EPI adsorbed at equilibrium and time  
48  
49 314  $t$  (min), respectively, and  $K_2$  is the equilibrium rate constant for pseudo-second-order  
50  
51 315 model. The  $Q_e$  and  $K_2$  value can be calculated from the slope and intercept of the linear  
52  
53 316 plot of  $t/Q_t$  versus  $t$ .

54  
55  
56 317 The parameters calculated are listed in Table 1. A plot of  $t/Q_t$  versus  $t$  was obtained  
57  
58 318 as a straight line with high correlation coefficient, which showed that the adsorption  
59  
60 319 process of EPI followed pseudo-second-order kinetic model. Furthermore, the amounts  
320 of drug adsorbed at equilibrium ( $Q_e$ ) calculated according to the pseudo-second-order

1  
2  
3  
4 321 model were more in accordance with the experimental data, which also indicated that  
5  
6 322 the adsorption of EPI onto M-MIPs could be better described by the pseudo-second-  
7  
8 323 order model than the first one.

9  
10 324 The initial adsorption rate ( $h_2$ ,  $\text{mg g}^{-1} \text{min}^{-1}$ ) were calculated according to the  
11  
12 325 following equation<sup>32</sup>:

13  
14  
15 326 
$$h_2 = K_2 Q_e^2 \quad (4)$$
  
16  
17

18 327 The rate constant ( $K_2$ ) depended on the surface coverage fraction of the drugs, which  
19  
20 328 was a complex function of the initial concentration of the solution<sup>33</sup>. The  $h_2$  value  
21  
22 329 calculated was 5.16 and 21.32 for M-MIPs and M-NIPs, respectively, which was a  
23  
24 330 verification of our former explanation that there was no imprinted cavity or specific  
25  
26 331 binding site inside M-NIPs, the adsorption was fast taking place only on the nonspecific  
27  
28 332 imprinted site of the polymers.

29  
30  
31 333 Based on the higher correlation coefficient ( $R^2$ ) values which approached unity and  
32  
33 334 the lower relative error, the pseudo-second-order model was therefore the most suitable  
34  
35 335 equation to describe the adsorption kinetic of EPI on the binding sites of M-MIPs. This  
36  
37 336 suggested that the overall rate of the adsorption process was controlled by  
38  
39 337 chemisorption<sup>34</sup>. Epirubicin molecules were strongly held onto the binding sites of M-  
40  
41 338 MIPs by several hydrogen bonds. On account of the strength and specificity of the  
42  
43 339 hydrogen bonds involved, the adsorption process was better described as chemisorption  
44  
45 340 than as physisorption<sup>32</sup>.

46  
47  
48 341 The pseudo-second-order model considered that all the steps of adsorption such as  
49  
50 342 external diffusion and internal diffusion were mixed together, which was not able to  
51  
52 343 identify the diffusion procedure. In order to study the adsorption mechanism, the intra-  
53  
54 344 particle diffusion model based on the theory proposed by Weber and Morris was  
55  
56 345 applied<sup>32</sup>. The intra-particle diffusion model is explored by the following equation:

57  
58  
59 346 
$$Q_t = K_i t^{0.5} + C_i \quad (5)$$
  
60

1  
2  
3  
4 347 where  $Q_t$  is the amount ( $\mu\text{g mg}^{-1}$ ) of EPI adsorbed at time  $t$  (min),  $K_i$  is the intra-  
5  
6 348 particle diffusion rate constant ( $\text{mg g}^{-1} \text{min}^{-1}$ ), which is obtained from the slope of the  
7  
8 349 straight line of  $Q_t$  versus  $t^{0.5}$ .  $C_i$  is the intercept of the line, represents the thickness of  
9  
10 350 the boundary layer. A larger  $C_i$  means a greater effect of boundary layer<sup>34</sup>. If the plot of  
11  
12 351  $Q_t$  versus  $t^{0.5}$  is a single line which passes through the origin, then the intra-particle  
13  
14 352 diffusion is the sole rate-limiting step. However, the data obtained from this study  
15  
16 353 exhibited a multi-linear plot, indicating that some other step was involved during the  
17  
18 354 adsorption process. Regarding the adsorption on M-MIPs, the plot could be divided into  
19  
20 355 three stages (Fig. 4): an initial sharp rise step was followed by a gradual increase stage  
21  
22 356 and a final plateau. The first step represented the external boundary adsorption which  
23  
24 357 ascribed to the diffusion of EPI through the solution to the external surface of M-MIPs<sup>35</sup>  
25  
26 358 and the fast uptake of the most available sites on the external surface of M-MIPs<sup>36</sup>. The  
27  
28 359 second step, namely the gradual adsorption stage, attributed to the intra-particle  
29  
30 360 diffusion when EPI transferred from the solution to the interior of M-MIPs. The plateau  
31  
32 361 phase corresponded to the final equilibrium state where the migration of EPI started to  
33  
34 362 slow down owing to the low concentration of EPI left in the solution. The plot of M-  
35  
36 363 NIPs was divided into two parts (Fig. 4): the initial rapid rise portion reflected the  
37  
38 364 external surface adsorption while the plain represented the final equilibrium stage. In  
39  
40 365 the overall adsorption process, the adsorption rate was fast in the initial phase and  
41  
42 366 slowed down with time elapsing. Moreover, it can be seen in Fig. 4, only the first parts  
43  
44 367 of the plots passed through the origin, suggesting that the intra-particle diffusion may  
45  
46 368 not be the sole rate limiting factor in the adsorption process, both external surface  
47  
48 369 diffusion and intra-particle diffusion contributed to the adsorption mechanism<sup>37</sup>.

#### 51 370 3.4. Adsorption isotherm study

52  
53  
54 371 Static adsorption tests were performed on 4.0 mg M-MIPs or M-NIPs with different  
55  
56 372 initial concentrations of the EPI solution. The adsorption isotherm plotted in Fig. 5  
57  
58 373 indicates that in the certain range of concentrations ( $5.0\text{-}50.0 \mu\text{g mL}^{-1}$ ), the amount of  
59  
60 374 EPI bound to M-MIPs and M-NIPs at adsorption equilibrium rose with the increasing  
375 of initial concentration of EPI. In addition, the amount of EPI adsorbed by M-MIPs was



1  
2  
3  
4 376 higher than that by M-NIPs. Several adsorption models were employed to study the  
5  
6 377 adsorption isotherm<sup>38</sup>.

7  
8  
9 378 The Langmuir isotherm model which assumes uniform adsorption on the surface of  
10  
11 379 the sorbent was used to describe monolayer adsorption on a surface containing a finite  
12  
13 380 number of binding sites with identical affinity<sup>35</sup>. The linear form of the equation is  
14  
15 381 expressed as:

16  
17  
18 382 
$$\frac{C_e}{Q_e} = \frac{C_e}{Q_m} + \frac{1}{Q_m K_L} \quad (6)$$
  
19  
20

21 383 where  $C_e$  is the equilibrium concentration ( $\mu\text{g mL}^{-1}$ ) of EPI in the bulk solution,  $Q_e$  is  
22  
23 384 the equilibrium adsorption capacity ( $\mu\text{g mg}^{-1}$ ),  $Q_m$  is the maximum adsorption capacity  
24  
25 385 ( $\mu\text{g mg}^{-1}$ ) which represents the total number of the binding sites,  $K_L$  is the Langmuir  
26  
27 386 constant ( $\text{mL } \mu\text{g}^{-1}$ ) related to the affinity of the binding sites.

28  
29  
30 387 The Langmuir isotherm equation can be expressed by a dimensionless constant called  
31  
32 388 separation factor or equilibrium parameter  $R_L$ , which is defined as follows:

33  
34  
35 389 
$$R_L = \frac{1}{1 + K_L C_0} \quad (7)$$
  
36  
37

38 390 where  $C_0$  is the initial concentration ( $\mu\text{g mL}^{-1}$ ) of EPI. The parameter  $R_L > 1$ ,  $R_L = 1$ , 0  
39  
40 391  $< R_L < 1$ ,  $R_L = 0$  indicates the isotherm shape according to unfavorable, linear, favorable  
41  
42 392 and irreversible, respectively<sup>39</sup>.

43  
44  
45 393 The Langmuir adsorption model is based on the assumption that the surface of the  
46  
47 394 sorbent is relatively homogeneous. In contrast, the continuous Freundlich model  
48  
49 395 describes the adsorption on a heterogeneous surface which supports binding sites with  
50  
51 396 varied affinities. The linear form of the isotherm equation is expressed as:

52  
53  
54  
55 397 
$$\log Q_e = m \log C_e + \log K_F \quad (8)$$
  
56  
57

58 398 where  $K_F$  is an indicative constant ( $\mu\text{g mg}^{-1}$ ) for adsorption capacity of the sorbent and  
59  
60 399  $m$  is known as the adsorption intensity or surface heterogeneity index. The value of  $m$

1  
2  
3  
4 400 should be between 0 and 1, which approaching to 0 increases the heterogeneous  
5  
6 401 character of the sorbent and equal to 1 represents to homogeneous materials.  
7  
8

9 402 The static adsorption data of EPI bound on M-MIPs and M-NIPs were analyzed by  
10  
11 403 Langmuir and Freundlich models. The values of correlation coefficient ( $R^2$ ) and the  
12  
13 404 parameters obtained from the two models are summarized in Table 2.  
14  
15

16 405 The calculated  $R_L$  values were between 0 and 1, which indicated a favorable  
17  
18 406 adsorption of EPI on M-MIPs and M-NIPs at the studied concentrations. The adsorption  
19  
20 407 isotherm of EPI on M-MIPs was better fitted by Freundlich adsorption model ( $R^2 >$   
21  
22 408 0.999) while that on M-NIPs was more suited to Langmuir adsorption model ( $R^2 >$   
23  
24 409 0.999), although the contrasted model also showed good agreement ( $R^2 > 0.980$ ).  
25  
26

27 410 For another point of view, the Langmuir model is suitable for a homogeneous surface,  
28  
29 411 while the Freundlich model is basically intended for a highly heterogeneous system,  
30  
31 412 being the system more heterogeneous as the  $m$  value is closer to 0. The experimental  
32  
33 413 data of M-MIPs ( $m < 0.4$ ) proved the heterogeneity of the surface of M-MIPs. This was  
34  
35 414 the consequence of the use of the high amount of functional monomer under non-  
36  
37 415 covalent imprinting conditions, with which the resulting M-MIPs contained a mixture  
38  
39 416 of binding cavities of diverse affinity for the template molecule<sup>40</sup>. In parallel, the  $m$   
40  
41 417 value of M-NIPs ( $m > 0.5$ ) suggested that although some degree of heterogeneity was  
42  
43 418 existed, a more homogeneous surface could be assumed.  
44  
45

46 419 In conclusion, M-MIPs had better applicability for the Freundlich adsorption model  
47  
48 420 while M-NIPs for Langmuir model, indicating that M-MIPs contained heterogeneous  
49  
50 421 binding sites and the surface of M-NIPs was homogeneous.  
51  
52

### 53 54 422 3.5. Selectivity study 55 56

57 423 Gatifloxacin was chosen as a reference compound to study the selectivity due to its  
58  
59 424 different structure with ANTs. Electronic Supplementary Information Fig. S3 illustrates  
60  
425 the adsorption capacity of M-MIPs and M-NIPs for these three structurally similar

1  
2  
3  
4 426 ANTs and the reference compound GTFX. It was obvious that the adsorption ability of  
5  
6 427 M-MIPs was much higher than that of M-NIPs. In addition, the adsorption ability of  
7  
8 428 the M-MIPs for these three ANTs was apparently higher than that of GTFX. Low  
9  
10 429 adsorption capacity of M-MIPs for GTFX was observed because of the different  
11  
12 430 structure compared with EPI. This result indicated that as to the substance which had  
13  
14 431 significantly different structures with the template molecule, there was no specific site  
15  
16 432 for it in the M-MIPs<sup>41</sup>.

17  
18  
19 433 To further investigate the adsorption ability of M-MIPs for different compounds  
20  
21 434 under competitive condition, the distribution coefficient ( $K_d$ ), the selectivity coefficient  
22  
23 435 ( $K$ ) and relative selectivity coefficient ( $K'$ ) were calculated. The equations of these  
24  
25 436 coefficients were interpreted in Electronic Supplementary Information Appendix S4.  
26  
27 437 The measured values are shown in Table 3.

28  
29  
30 438 The distribution coefficient  $K_d$  is a reflection of the adsorption capacity. A larger  
31  
32 439 value of  $K_d$  suggests a stronger adsorption capacity of M-MIPs to the substance. The  
33  
34 440 selectivity coefficient  $K$  represents the difference in the adsorption capacity of the same  
35  
36 441 sorbent to different substances, while the relative selectivity coefficient  $K'$  represents  
37  
38 442 the discrepancy between different sorbents. As can be seen in Table 3, M-MIPs had  
39  
40 443 high discriminatory power between ANTs and the reference GTFX.

### 41 42 43 44 444 3.6. Optimization of SPE procedure

45  
46  
47 445 The conditions of M-MIPs amount, adsorption time and elution solvent were analyzed.  
48  
49 446 As shown in Electronic Supplementary Information Fig. S4, best recoveries were  
50  
51 447 obtained when 3.0 mg of M-MIPs was added. Electronic Supplementary Information  
52  
53 448 Fig. S5 indicates that 45 min was sufficient to achieve satisfactory recoveries. Further  
54  
55 449 increasing of the adsorption time did not result in improved recoveries. As can be seen  
56  
57 450 in Electronic Supplementary Information Fig. S6, using methanol-acetic acid (8:2, v/v)  
58  
59 451 as the elution solvent was enough and high recoveries were obtained.

### 60 452 3.7. Validation of the magnetic MISPE-HPLC method

1  
2  
3  
4 453 The analytical performance of the magnetic MISPE-HPLC method was evaluated with  
5  
6 454 a series of spiked urine samples. The linear range of the method was in the range of  
7  
8 455 0.01-20.0  $\mu\text{g mL}^{-1}$ , with correlation coefficient 0.9991 for DOX and 0.9994 for DAUN.  
9  
10 456 The LOD (limit of detection) and LOQ (limit of quantification) were obtained from the  
11  
12 457 diluted samples and the signal-to-noise ratio (S/N). According to the experiment results,  
13  
14 458 the LOD (S/N = 3) and LOQ (S/N = 10) were 0.6  $\text{ng mL}^{-1}$  and 1.0  $\text{ng mL}^{-1}$  for DOX,  
15  
16 459 and 2.4  $\text{ng mL}^{-1}$  and 5.0  $\text{ng mL}^{-1}$  for DAUN, respectively. The enrichment factor was  
17  
18 460 10.

19  
20  
21 461 The precision of the method was investigated in terms of the intraday repeatability  
22  
23 462 (the experiments were repeated 6 times) and interday reproducibility (6 different days)  
24  
25 463 using 0.1, 1.0 and 10.0  $\mu\text{g mL}^{-1}$  concentration levels for each analyte in the urine  
26  
27 464 samples. The intraday repeatability was evaluated as the relative standard deviation  
28  
29 465 (RSD) ranged from 0.3% to 3.2% and the interday reproducibility was less than 8% in  
30  
31 466 all cases. The variations in the precision of the method might be due to the small amount  
32  
33 467 of sample used.

### 36 468 3.8. Simultaneous determination of DOX and DAUN in urine samples

37  
38  
39 469 Urine samples spiked with different concentrations of DOX and DAUN (0.1, 1.0 and  
40  
41 470 10.0  $\mu\text{g mL}^{-1}$ ) were tested to evaluate the accuracy and applicability of the method. At  
42  
43 471 each concentration, five independent measurements were implemented. The results  
44  
45 472 were listed in Electronic Supplementary Information Table S1. The calculated  
46  
47 473 recoveries of DOX and DAUN in the urine samples ranged from 93.9%  $\pm$  5.2% to 100.0%  
48  
49 474  $\pm$  3.4%. As shown in Fig. 6, M-MIPs (Fig. 6a) performed much better than M-NIPs  
50  
51 475 (Fig. 6b) when extracted DOX and DAUN from spiked urine samples. The results  
52  
53 476 indicated the practical applicability of the method in this study for the simultaneous  
54  
55 477 extraction and determination of ANTs from urine samples. Table 4 summarizes the  
56  
57 478 performance of this method and other techniques reported in literatures<sup>3, 5, 11</sup>,  
58  
59 479 respectively. Compared with the other methods, the simple method we proposed  
60

1  
2  
3  
4 480 displays high sensitivity, low detection limits, appropriate linear range and satisfactory  
5  
6 481 recovery without the use of expensive instruments.  
7

### 8 9 482 *3.9. Reusability of M-MIPs*

10  
11 483 The character of reusability is one of the outstanding advantages of M-MIPs, which  
12  
13 484 makes the material an economical sorbent for SPE. Five adsorption-desorption cycles  
14  
15 485 were performed in this study to investigate the regeneration of M-MIPs. The relative  
16  
17 486 recovery fluctuated from 90.8% to 97.6%, which was no significant loss in adsorption  
18  
19 487 capacity. The property of M-MIPs obtained in this study was stable in the bio-matrix  
20  
21 488 samples.  
22  
23  
24

### 25 489 **Conclusion**

26  
27  
28 490 In this study, M-MIPs using EPI as dummy template were prepared by imprinting on  
29  
30 491 the surface of Fe<sub>3</sub>O<sub>4</sub> nanoparticles for simultaneous extraction and pre-concentration of  
31  
32 492 ANTs from urine. The proposed method overcame the problems of the traditional  
33  
34 493 methods, such as the the potential risk of residual templates leakage, packing of the SPE  
35  
36 494 column and the tedious centrifugation and filtration, thus ensured the reliability and  
37  
38 495 simplified the sample pretreatment process. The adsorption mechanism of the  
39  
40 496 synthesized polymers was investigated in detail for the first time. The research of  
41  
42 497 selectivity showed that compounds with the identical structure as the template could be  
43  
44 498 recognized and extracted simultaneously, which saved much time and cost in multiple  
45  
46 499 sample prertreatment. The successful application in the simultaneous enrichment and  
47  
48 500 determination of ANTs in urine samples indicated that the water-compatible M-MIPs  
49  
50 501 coupled to the HPLC could be a promising tool in the analysis of these therapeutic  
51  
52 502 agents from biological fluids.  
53  
54  
55

56 503 **Acknowledgments** This work was supported by Guizhou Provincial Natural Science  
57  
58 504 Foundation of China (Grant No. 20122288), the Graduate Students Innovative Projects  
59  
60 505 of Jiangsu Province (Program No. CXZZ11\_0812) and by the National Basic Science

1  
2  
3  
4 506 Personal Training Fund (No. J0630858). The authors are delighted to acknowledge  
5  
6 507 discussions with colleagues in their research group.  
7  
8

9 508 **References**

- 10  
11  
12 509 1. S. N. Mahnik, B. Rizovski, M. Fuerhacker and R. M. Mader, *Chemosphere*, 2006, 65,  
13 510 1419-1425.  
14 511 2. H. Lu, G. Yuan, Q. He and H. Chen, *Microchemical Journal*, 2009, 92, 170-173.  
15 512 3. Q. Hu, L. Zhang, T. Zhou and Y. Fang, *Analytica Chimica Acta*, 2000, 416, 15-19.  
16 513 4. Z. Chen, S. Qian, G. Liu, X. Chen and J. Chen, *Microchimica Acta*, 2011, 175, 217-223.  
17 514 5. F. Martínez Ferreras, O. S. Wolfbeis and H. H. Gorris, *Analytica Chimica Acta*, 2012,  
18 515 729, 62-66.  
19 516 6. M. Pieri, L. Castiglia, P. Basilicata, N. Sannolo, A. Acampora and N. Miraglia, *Annals of*  
20 517 *Occupational Hygiene*, 2010, 54, 368-376.  
21 518 7. K. E. Maudens, C. P. Stove, V. F. J. Cocquyt, H. Denys and W. E. Lambert, *Journal of*  
22 519 *Chromatography B*, 2009, 877, 3907-3915.  
23 520 8. S. Ahmed, N. Kishikawa, K. Ohyama, M. Wada, K. Nakashima and N. Kuroda, *Talanta*,  
24 521 2009, 78, 94-100.  
25 522 9. S. Nussbaumer, L. Geiser, F. Sadeghipour, D. Hochstrasser, P. Bonnabry, J.-L. Veuthey  
26 523 and S. Fleury-Souverain, *Analytical and Bioanalytical Chemistry*, 2011, 402, 2499-2509.  
27 524 10. C. Sottani, P. Rinaldi, E. Leoni, G. Poggi, C. Teragni, A. Delmonte and C. Minoia, *Rapid*  
28 525 *Communications in Mass Spectrometry*, 2008, 22, 2645-2659.  
29 526 11. C. Sottani, G. Tranfo, M. Bettinelli, P. Faranda, M. Spagnoli and C. Minoia, *Rapid*  
30 527 *Communications in Mass Spectrometry*, 2005, 18, 2426-2436.  
31 528 12. T. Hu, Q. Le, Z. Wu and W. Wu, *Journal of Pharmaceutical and Biomedical Analysis*,  
32 529 2007, 43, 263-269.  
33 530 13. A. L. Sanson, S. C. R. Silva, M. C. G. Martins, A. Giusti-Paiva, P. P. Maia and I. Martins,  
34 531 *Brazilian Journal of Pharmaceutical Sciences*, 2011, 47, 363-371.  
35 532 14. P. Dramou, P. Zuo, H. He, L. A. Pham-Huy, W. Zou, D. Xiao, C. Pham-Huy and T. Ndorbor,  
36 533 *Journal of Materials Chemistry B*, 2013, 1, 4099-4109.  
37 534 15. Q. Zhang, L. Zhang, P. Wang and S. Du, *Journal of pharmaceutical sciences*, 2014. DOI  
38 535 10.1002/jps.23838  
39 536 16. F. F. Chen, R. Wang and Y. P. Shi, *Talanta*, 2012, 89, 505-512.  
40 537 17. N. Li, T. B. Ng, J. H. Wong, J. X. Qiao, Y. N. Zhang, R. Zhou, R. R. Chen and F. Liu, *Food*  
41 538 *Chemistry*, 2013, 139, 1161-1167.  
42 539 18. L. Mergola, S. Scorrano, R. Del Sole, M. R. Lazzoi and G. Vasapollo, *Biosensors and*  
43 540 *Bioelectronics*, 2013, 40, 336-341.  
44 541 19. Z. Zhang, W. Tan, Y. Hu, G. Li and S. Zan, *Analyst*, 2012, 137, 968-977.  
45 542 20. Y. Zhang, R. Liu, Y. Hu and G. Li, *Analytical Chemistry*, 2009, 81, 967-976.  
46 543 21. M. Bouri, M. J. Lerma-García, R. Salghi, M. Zougagh and A. Ríos, *Talanta*, 2012, 99,  
47 544 897-903.  
48 545 22. J. Zhan, G. Fang, Z. Yan, M. Pan, C. Liu and S. Wang, *Analytical and Bioanalytical*  
49 546 *Chemistry*, 2013, 405, 6353-6363.

- 1  
2  
3 547 23. D. Xiao, P. Dramou, N. Xiong, H. He, D. Yuan, H. Dai, H. Li, X. He, J. Peng and N. Li,  
4 548 *Analyst*, 2013, 138, 3287-3296.
- 5 549 24. H. Yan, K. H. Row and G. Yang, *Talanta*, 2008, 75, 227-232.
- 6 550 25. G. Qu, S. Zheng, Y. Liu, W. Xie, A. Wu and D. Zhang, *Journal of Chromatography B*,  
7 551 2009, 877, 3187-3193.
- 8 552 26. M. Singh, A. Kumar and N. Tarannum, *Analytical and Bioanalytical Chemistry*, 2013,  
9 553 405, 4245-4252.
- 10 554 27. K. Hua, L. Zhang, Z. Zhang, Y. Guo and T. Guo, *Acta Biomaterialia*, 2011, 7, 3086-3093.
- 11 555 28. P. Dramou, D. Xiao, H. He, T. Liu and W. Zou, *Journal of Separation Science*, 2013, 36,  
12 556 898-906.
- 13 557 29. D. Xiao, P. Dramou, N. Xiong, H. He, H. Li, D. Yuan, H. Dai, *Journal of chromatography*  
14 558 *A*, 2013, 1274, 44-53.
- 15 559 30. X. Wang, H. Mao, W. Huang, W. Guan, X. Zou, J. Pan and Y. Yan, *Chemical Engineering*  
16 560 *Journal*, 2011, 178, 85-92.
- 17 561 31. W. Guo, W. Hu, J. Pan, H. Zhou, W. Guan, X. Wang, J. Dai and L. Xu, *Chemical*  
18 562 *Engineering Journal*, 2011, 171, 603-611.
- 19 563 32. M. C. Cela-Perez, M. M. Castro-Lopez, A. Lasagabaster-Latorre, J. M. Lopez-Vilarino,  
20 564 M. V. Gonzalez-Rodriguez and L. F. Barral-Losada, *Analytica Chimica Acta*, 2011, 706,  
21 565 275-284.
- 22 566 33. S. Azizian, *Journal of Colloid and Interface Science*, 2004, 276, 47-52.
- 23 567 34. I. A. W. Tan, A. L. Ahmad and B. H. Hameed, *Journal of Hazardous Materials*, 2009,  
24 568 164, 473-482.
- 25 569 35. J. Pan, X. Zou, X. Wang, W. Guan, Y. Yan and J. Han, *Chemical Engineering Journal*,  
26 570 2010, 162, 910-918.
- 27 571 36. M. Lopez Mdel, M. C. Perez, M. S. Garcia, J. M. Vilarino, M. V. Rodriguez and L. F.  
28 572 Losada, *Analytica Chimica Acta*, 2012, 721, 68-78.
- 29 573 37. W. Liu, J. Zhang, C. Zhang, Y. Wang and Y. Li, *Chemical Engineering Journal*, 2010, 162,  
30 574 677-684.
- 31 575 38. J. A. García-Calzón and M. E. Díaz-García, *Sensors and Actuators B: Chemical*, 2007,  
32 576 123, 1180-1194.
- 33 577 39. T. Y. Guo, Y. Q. Xia, G. J. Hao, M. D. Song and B. H. Zhang, *Biomaterials*, 2004, 25, 5905-  
34 578 5912.
- 35 579 40. R. J. Umpleby II, S. C. Baxter, M. Bode, J. K. Berch Jr, R. N. Shah and K. D. Shimizu,  
36 580 *Analytica Chimica Acta*, 2001, 435, 35-42.
- 37 581 41. F. F. Chen, X. Y. Xie and Y. P. Shi, *Journal of Chromatography A*, 2013, 1300, 112-118.  
38 582
- 39 583
- 40 584
- 41 585
- 42 586

## Figure Captions

587  
588 **Fig. 1** SEM image (a) and TEM image (b) of M-MIPs. Scale bars: 300 nm for (a) and  
589 100 nm for (b).

590 **Fig. 2** Magnetization curves of Fe<sub>3</sub>O<sub>4</sub> and M-MIPs (a) and the magnetic performance  
591 of M-MIPs within a few seconds using an external magnetic field (b)

592 **Fig. 3** Adsorption kinetic curves for EPI on M-MIPs and M-NIPs (EPI: initial  
593 concentration: 10.0 µg mL<sup>-1</sup>, volume: 50.0 mL; M-MIPs or M-NIPs amount: 50.0 mg;  
594 adsorption time: 0 min to 180 min)

595 **Fig. 4** Plot of intra-particle diffusion model for adsorption of EPI on M-MIPs and M-  
596 NIPs (EPI: initial concentration: 10.0 µg mL<sup>-1</sup>, volume: 50.0 mL; M-MIPs or M-NIPs  
597 amount: 50.0 mg; adsorption time: 0 min to 180 min)

598 **Fig. 5** Adsorption isotherm curves for EPI on M-MIPs and M-NIPs (EPI: concentration:  
599 5.0 µg mL<sup>-1</sup> - 50.0 µg mL<sup>-1</sup>, volume: 4.0 mL; M-MIPs or M-NIPs amount: 4.0 mg)

600 **Fig. 6** Magnetic MISPE-HPLC chromatograms of DOX and DAUN (both 0.1 µg mL<sup>-1</sup>  
601 <sup>1</sup>) which were spiked in urine samples and extracted by EPI-M-MIPs (a) and EPI-M-  
602 NIPs (b) (urine samples: 4.0 mL, M-MIPs or M-NIPs amount: 3.0 mg)

603

604

605

606

607

608

609

610



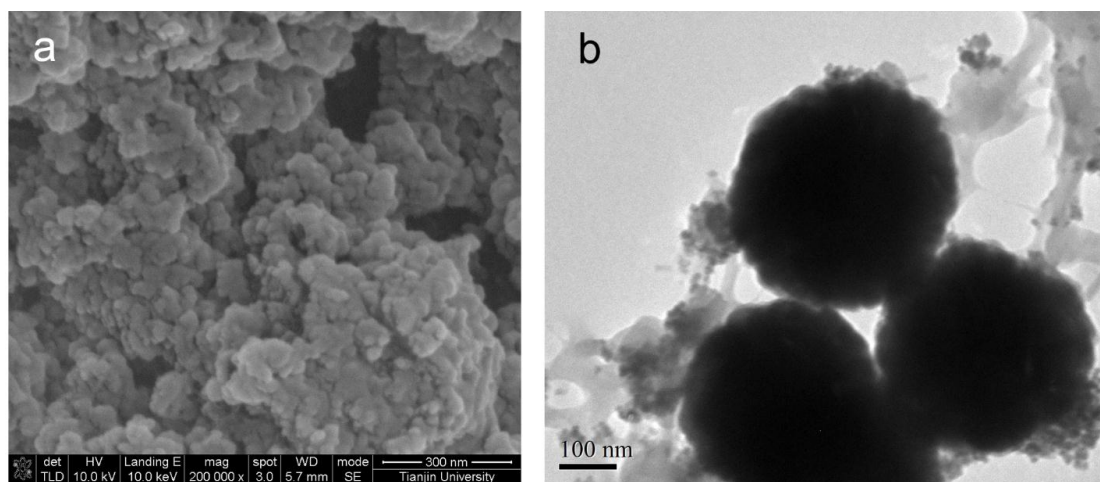


Fig. 1

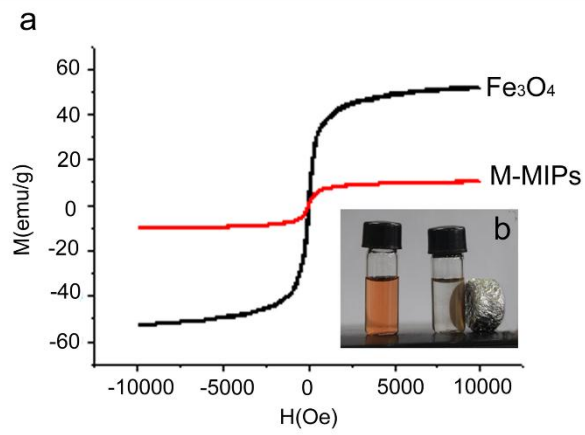


Fig. 2

614

615

616

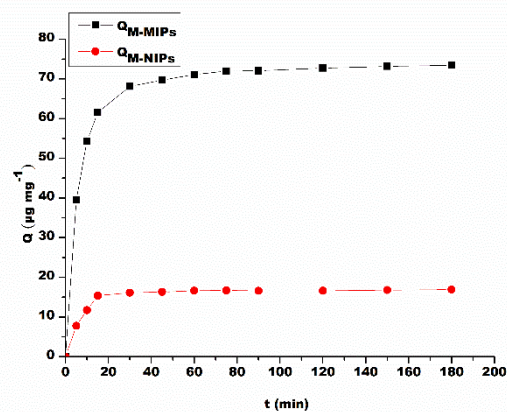


Fig. 3

617

618

619

1  
2  
3  
4  
5  
6  
7  
8  
9  
10  
11  
12  
13  
14  
15  
16  
17  
18  
19  
20  
21  
22  
23  
24  
25  
26  
27  
28  
29  
30  
31  
32  
33  
34  
35  
36  
37  
38  
39  
40  
41  
42  
43  
44  
45  
46  
47  
48  
49  
50  
51  
52  
53  
54  
55  
56  
57  
58  
59  
60

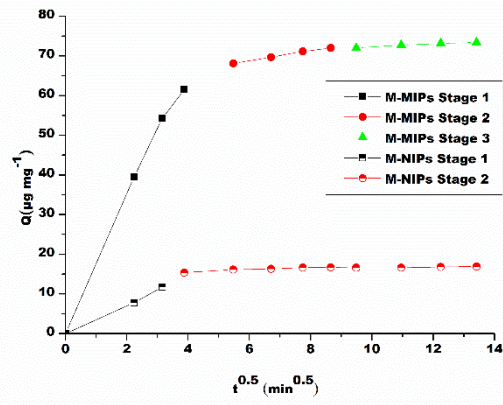


Fig. 4

620

621

622

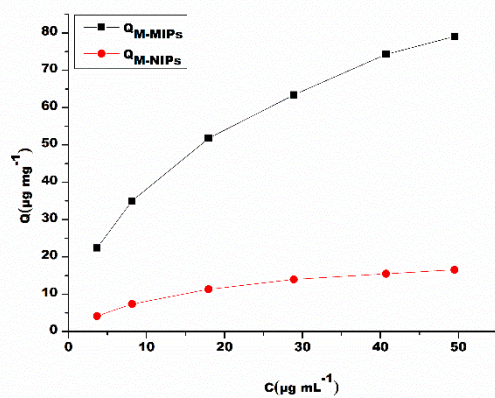


Fig. 5

623

624

625

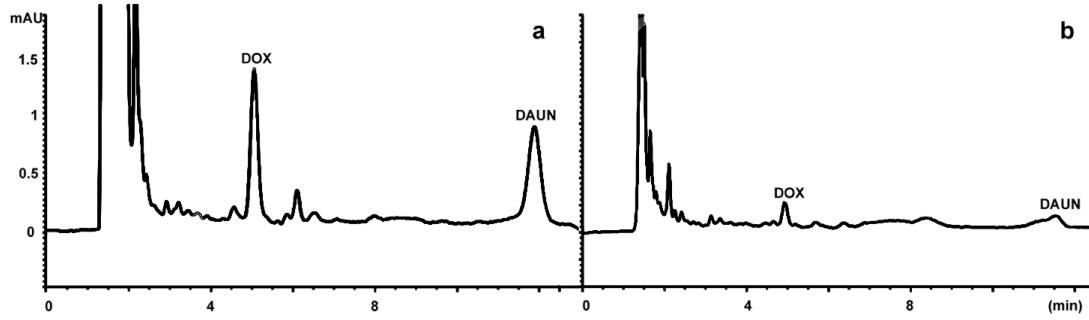


Fig. 6

626

627

628

1  
2  
3  
4  
5  
6  
7  
8  
9  
10  
11  
12  
13  
14  
15  
16  
17  
18  
19  
20  
21  
22  
23  
24  
25  
26  
27  
28  
29  
30  
31  
32  
33  
34  
35  
36  
37  
38  
39  
40  
41  
42  
43  
44  
45  
46  
47  
48  
49  
50  
51  
52  
53  
54  
55  
56  
57  
58  
59  
60

629 **Table 1** Adsorption kinetic constants of the pseudo-first-order model and pseudo-second-order  
 630 model for M-MIPs and M-NIPs

Materials	$Q_{e,exp}$ ( $\mu\text{g mg}^{-1}$ )	Pseudo-first-order kinetic model				Pseudo-second-order kinetic model			
		$Q_{e,cal}$ ( $\mu\text{g mg}^{-1}$ )	$K_1$ ( $\text{min}^{-1}$ )	$R_1^2$	Relative error (%)	$Q_{e,cal}$ ( $\mu\text{g mg}^{-1}$ )	$K_2$ ( $\text{g mg}^{-1} \text{min}^{-1}$ )	$R_2^2$	Relative error (%)
M-MIPs	73.45	26.12	0.0329	0.9133	64.44	75.19	0.0037	1	2.37
M-NIPs	16.92	3.06	0.0252	0.7332	81.91	17.24	0.0174	0.9995	1.89

631

632

633

634

635

636

637

638

639

640

641

642

643 **Table 2** Langmuir and Freundlich adsorption model parameters and correlation coefficient for EPI  
644 bound on M-MIPs and M-NIPs at 25 °C

Materials	Langmuir adsorption model				Freundlich adsorption model		
	$Q_m$ ( $\mu\text{g mg}^{-1}$ )	$K_L$ ( $\text{mL } \mu\text{g}^{-1}$ )	$R_L$	$R^2$	$K_F$ ( $\mu\text{g mg}^{-1}$ )	$m$	$R^2$
M-MIPs	89.29	0.14	0.60-0.95	0.9849	19.52	0.3797	0.9996
M-NIPs	21.10	0.07	0.22-0.80	0.9992	2.49	0.5082	0.9805

645

646

647

648

649

650

651

652

653

654

655

656

657

658



659 **Table 3** The selectivity parameters of the M-MIPs and M-NIPs

Analyte	Distribution coefficient <sup>a</sup> ,		Selectivity coefficient <sup>b</sup> ,		Relative selectivity coefficient <sup>c</sup> , K'
	K <sub>d</sub> (mL mg <sup>-1</sup> )		K		
	M-MIPs	M-NIPs	M-MIPs	M-NIPs	
EPI	1.26	0.14	9.72	1.32	7.38
DOX	1.26	0.13	9.75	1.20	8.12
DAUN	1.72	0.20	13.31	1.85	7.18
GTFX	0.13	0.11			

660 <sup>a</sup>Distribution coefficient:  $K_d = \frac{Q}{c_e}$

661 <sup>b</sup>Selectivity coefficient:  $K = \frac{K_d(\text{ANTS})}{K_d(\text{GTFX})}$

662 <sup>c</sup>Relative selectivity coefficient:  $K' = \frac{K_{\text{M-MIPs}}}{K_{\text{M-NIPs}}}$

663

664

665

666

667

668

669

670

671

672

673

674

675 **Table 4** Determination of ANTs in urine samples with different methods

Method	Analytes	Linear Range ( $\mu\text{g mL}^{-1}$ )	LOD ( $\text{ng mL}^{-1}$ )	Recovery (%)	RSD (%)	Reference
CZE-AD <sup>a</sup>	DAUN	1-100	400	93.2-109.0	$\leq 4.7$	3
DLR- fluorometry <sup>b</sup>	DOX	-	217	$\geq 97$	-	5
SPE-HPLC- MS/MS <sup>c</sup>	DOX, DAUN, EPI, IDA <sup>e</sup>	0.0001-0.002	0.01-0.04	79.1-102.0	$\leq 9.1$	11
M-MISPE- HPLC-UV <sup>d</sup>	DOX, DAUN	0.01-20.0	0.6-2.4	93.9-100.0	$\leq 6.7$	This work

676 <sup>a</sup>CZE-AD: capillary zone electrophoresis with amperometric detection.677 <sup>b</sup>DLR- fluorometry: dual lifetime referenced fluorometry.678 <sup>c</sup>SPE-HPLC-MS/MS: solid-phase extraction-high-performance liquid chromatography/tandem mass spectrometry.679 <sup>d</sup>M-MISPE-HPLC-UV: magnetic molecularly imprinted solid-phase extraction-high-performance liquid chromatography-ultraviolet  
680 detector.681 <sup>e</sup>IDA: Idarubicin

682

683

684

685

686

687

688

689